Influence of oxygen pressure on critical current density and magnetic flux pinning structures in $YBa_2Cu_3O_{7-x}$ fabricated by chemical solution deposition*

Ding Fa-Zhu(丁发柱)†, Gu Hong-Wei(古宏伟), Zhang Teng(张 腾), Dai Shao-Tao(戴少涛), and Xiao Li-Ye(肖立业)

Key Laboratory of Applied Superconductivity, Institute of Electrical Engineering, Chinese Academy of Sciences, Beijing 100190, *China*

(Received 1 September 2010; revised manuscript received 13 September 2010)

This paper studies the effect of oxygen partial pressure on the fabrication of $YBa_2Cu_3O_{7-x}$ films on (00l) $LaAlO_3$ substrates by metalorganic deposition using trifluoroacetates (TFA-MOD). As the oxygen partial pressure increases to 1500 Pa, a great increase in the superconducting properties is observed at high magnetic fields parallel to the YBCO c axis. The cross-sectional transmission electron microscope images show that a high density of stacking faults in the size range of 10–15 nm may act as flux pinning centres to enhance the critical current density of the YBCO films

Keywords: YBCO, oxygen pressure, stacking fault, TFA-MOD

PACS: 74.76.Bz, 81.15.Lm **DOI:** 10.1088/1674-1056/20/2/027402

1. Introduction

Remarkably there has been much interest recently in improving the magnetic flux pinning of $YBa_2Cu_3O_{7-x}$ (YBCO) films, driven by better performance and lower fabrication costs of YBCO wire. As the coherence length in high temperature superconductors is very small, only nanosized microstructure within the YBCO matrix can act as effective pinning centres.[1] Approaches to obtain significant improvements in critical current density (J_C) have been realized for YBCO films, including decoration of substrate surfaces by nanoparticles,[2−5] addition of oxide nanoparticles,[6−9] multilayering of YBCO with second-phase materials,[10,11] mixed rare-earth doping,[12−15] and an intentional deviation from the 123 stoichiometry.[16,17] In recent years, it was also reported that the high J_C of YBCO films was obtained by changing the growth parameters.[18−20] In this work, we examine the microstructure and critical current density of YBCO films prepared by TFA-MOD as a function of oxygen partial pressure. The YBCO films prepared at oxygen partial pressure of 1500 Pa showed the highest critical current density in magnetic field, which was attributed to a high density of stacking faults in the size range of 10 nm–15 nm.

2. Experimental details

The trifluoroacetate precursor solution for YBCO film was prepared by dissolving the acetates of yttrium, barium, and copper in a 1:2:3 cation ratio in de-ionized water with an excess stoichiometric quantity of trifluoroacetic acid at room temperature. The resulting aqueous solution was refluxed for 10 h and then dried to a semisolid state, and then re-dissolved in methanol for drying. Finally, the residue was dissolved in sufficient methanol to obtain the final trifluoroacetate precursor solution whose concentration was 1.5 mol/L. The solution was coated onto 10 mm×10 mm (00 h)-oriented $LaAlO_3$ (LAO) substrates at a spinning rate of 3000 rpm for 2 min. Then the samples were put in a quartz tube within a horizontal furnace. Coated films were calcined at the temperature up to 400 °C in 4.2% humidified oxygen with a flow rate of 500 cc/min. The calcined films were fired at 820 °C with 4.2% humidified Ar gas mixed with different content oxygen gas for 3 h and finally oxygenated at 500 °C for 1.5 h in a pure oxygen gas atmosphere. Different partial oxygen pressures were obtained by controlling the gas mass flowmeter. Consequently, YBCO films with thickness of 200 nm were obtained.

*Project supported by the National Natural Science Foundation of China (Grant No. 51002149).

†Corresponding author. E-mail: dingfazhu@mail.iee.ac.cn

© 2011 Chinese Physical Society and IOP Publishing Ltd

The surface morphology of the YBCO films were observed by field emission scanning electron microscope (SEM) (FESEM, FEI-Siron). The cross sections of the films were examined with a JOEL 201 transmission electron microscope (TEM) which is operated at 200 kV. The texture of the as-grown film was characterized by pole-figure analysis (Philips X' Pert MRD). The magnetic J_C measurements were made with a quantum design physical property measurement system (PPMS) vibrating sample magnetometer (VSM).

3. Results and discussion

Figure 1 compares the longitudinal J_C at 77 K of three YBCO films prepared at different oxygen pressures as a function of magnetic field (H). The magnetic field is applied parallelly to the c axis. The inset figure presents J_C as a function of oxygen partial pressure for self-field. It can be seen that the YBCO films prepared at oxygen pressure of 100–2000 Pa exhibit high critical current density. There is a large oxygen pressure window of at least 1900 Pa that maintains high J_C ($H = 0$) at the value of 3.5 MA/cm^2. However, with increasing the oxygen pressure (2500 Pa), the J_C of YBCO films drastically decreased to 0.63 MA/cm^2. Although no systematic J_C variation in self-field was observed (J_{C0} between 5.0 and 6.0 MA/cm^2), at higher magnetic fields, a distinct increase in J_C can be correlated with an increase in the oxygen pressure. For instance, the J_C value of YBCO films prepared at oxygen pressure of 1500 Pa is about 5.0 times at 1 T and 77 K larger than that of YBCO films prepared at oxygen pressure of 100 Pa. The dramatic change in the shape of J_C from oxygen partial pressure of 100 Pa to 1500 Pa is suggestive of the microstructure transition.

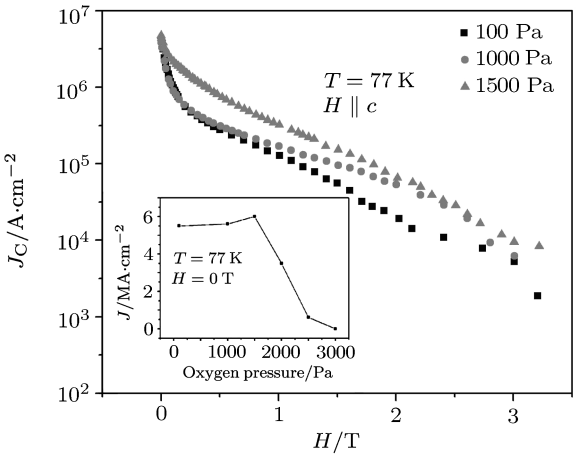


Fig. 1. Comparison of J_C versus magnetic field for $H \parallel c$ at 77 K for a series of YBCO films prepared at different oxygen pressure. The inset figure shows the dependence of self-field J_C (0 T, 77 K) on the oxygen pressure for YBCO films.

Figure 2 shows a typical cross-sectional high resolution (HR) TEM image of YBCO films prepared at oxygen pressure of 1500 Pa. We found a high density of stacking faults (as indicated by the white lines drawn on the micrograph), randomly distributed within the matrix. These stacking faults are 3 nm–5 nm in width and 10 nm–15 nm-long on average, which are the same as the order of the coherence length of YBCO. However, relative to the YBCO films grown at oxygen pressure of 100 Pa, there were no stacking faults.[21] Therefore, these stacking faults can act as effect of flux pinning centers to enhance the critical current density of the YBCO films.

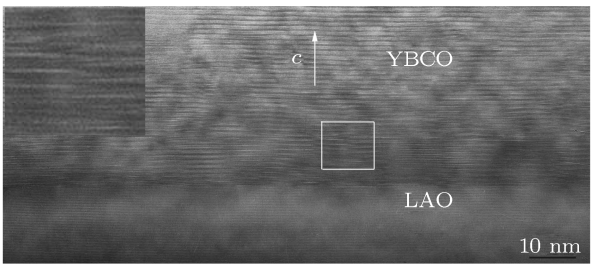


Fig. 2. Cross section HRTEM image of the sample YBCO film prepared at oxygen pressure of 2000 Pa, showing a large density of stacking faults.

Figure 3 shows the SEM micrographs of the YBCO thin films prepared at different oxygen pressures. We can observe the evolution of surface morphologies with different oxygen pressures. From Figs. 3(a)–3(c), the smooth and dense surface without any a-axis grains could be observed in the whole area of YBCO films fabricated at 100 Pa–1500 Pa of oxygen pressure. And with increasing the oxygen pressure, a few needle (a-axis) grains appeared in the YBCO films, as the arrow labeled in Fig. 3(d). Furthermore, it can be seen from Fig. 3(e) that more a-axis grains are easily identified due to their platelet-like shape and their orientation is parallel to the orthogonal (100) axes of the substrate.

For further verification, an analysis of the (102) pole-figure was conducted to evaluate the texture of the films. From Figs. 4(a) and 4(b), a fourfold symmetry can be clearly seen, which confirms that the YBCO films prepared at 1500 Pa–2000 Pa of oxygen pressure present primarily a single in-plane orientation. However, it can be seen from Fig. 4(c) that there are four symmetric (100) YBCO reflections besides four symmetric (001) YBCO reflections. It is concluded that

the YBCO films prepared at 2500 Pa of oxygen pressure have a-axis grains. The results agree well with the SEM analysis. Combining with Figs. 1 and 3, we find that the YBCO films prepared at high oxygen pressure (2500 Pa) evidently have lower J_C value due to a-axis grains.

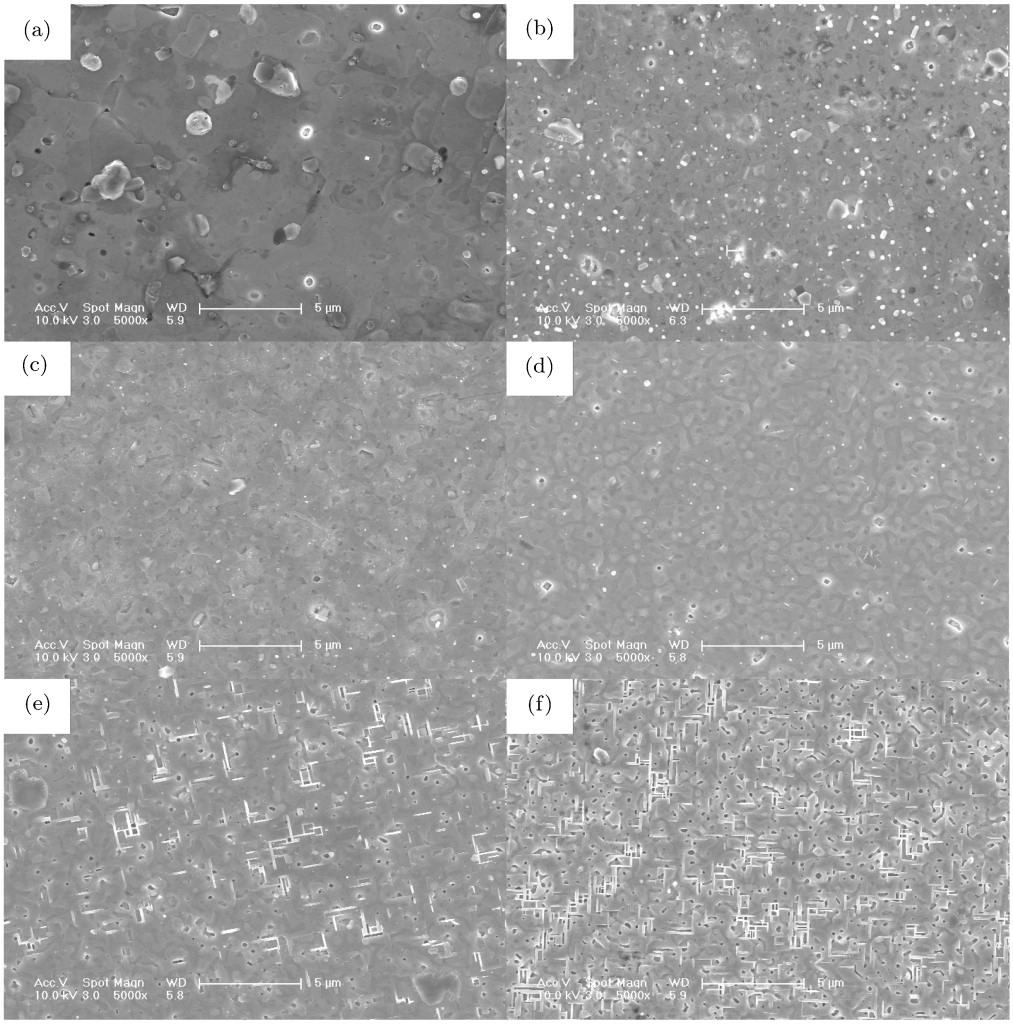


Fig. 3. The SEM micrograph of YBCO films with different oxygen pressures (a) 100 Pa; (b) 1000 Pa; (c) 1500 Pa; (d) 2000 Pa; (e) 2500 Pa and (f) 3000 Pa.

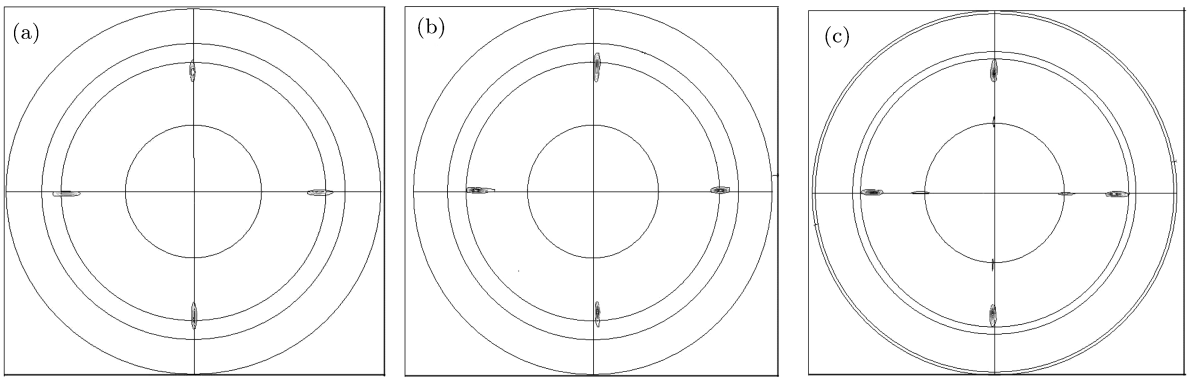


Fig. 4. The (102) pole figures of the YBCO film prepared at different oxygen pressures: (a) 1500 Pa; (b) 2000 Pa and (c) 2500 Pa.

All the results presented here demonstrate that the oxygen partial pressure is a key factor to modify the balance between the nucleation rate of c-axis and a-axis oriented grains at fixed growth temperatures. It is clear from Figs. 3 and 4 that the YBCO films prepared below 1000 Pa of oxygen pressure are completely crystallized with a pure YBCO (001) phase. Above 2000 Pa, a-axis oriented YBCO grains occur. We would like to stress the evolution of the microstructure of the YBCO films with oxygen pressure from 1000 Pa to 2000 Pa. During this range, some disorder occurs in the YBCO structure, as evidenced in the HRTEM displayed in Fig. 2 where the stacking faults were induced. Thus, the critical current density of YBCO films was improved.

4. Conclusions

In summary, we have examined the effect of oxygen pressure on YBCO films grown by TFA-MOD. It was found that the YBCO films prepared at oxygen pressure of 1500 Pa showed maximized $J_{\rm C}$ ($H \parallel c$) for 0.5 T–3 T due to a high density of stacking faults. And for self-field, the YBCO films prepared at oxygen pressure of 100 Pa–2000 Pa exhibited similar $J_{\rm C}$ (3.5 MA/cm^2). These results demonstrate that substantial improvements can be obtained by simply manipulating the defect structure that occurs naturally during growth of YBCO films. So, this approach offers an alternative method to enhance the applicability of YBCO coated conductors via a cost-effective route.

References

[1] Foltyn S R, Civale L, MacManus-Driscoll J L, Jia Q X, Maiorov B, Wang H and Maley M 2007 *Nature Mater.* **6** 631

[2] Crisan A, Fujiwara S, Nie J C, Sundaresan A and Ihara H 2001 *Appl. Phys. Lett.* **79** 4547

[3] Aytug T, Paranthaman M, Gapud A A, Kang S, Christen H M, Leonard K J, Martin P M, Thompson J R, Christen D K, Meng R, Rusakova I, Chu C W and Johansen T H 2005 *J. Appl. Phys.* **98** 114309

[4] Nie J C, Yamasaki H, Yamada H, Nakagawa Y, Develos-Bagarinao K and Mawatari Y 2004 *Supercond. Sci. Technol.* **17** 845

[5] Shi D Q, Ma P, Rock K Ko, Kim H S, Chung J K, Song K J and Chan P 2007 *Chin. Phys.* **16** 2142

[6] MacManus-Driscoll J L, Foltyn S R, Jia Q X, Wang H, Serquis A, Civale L, Maiorov B, Hawley M E, Maley M P and Peterson D E 2004 *Nature Mater.* **3** 439

[7] Baca F J, Barnes P N, Emergo R S, Haugan T J, Reichart J N and Wu J Z 2009 *Appl. Phys. Lett.* **94** 102512

[8] Varanasi C V, Barnes P N, Burke J, Brunke L, Maartense I, Haugan T J, Stinzianni E A, Dunn K A and Haldar P 2006 *Supercond. Sci. Technol.* **19** L37

[9] Zhou Y X, Ghalsasi S, Rusakova I and Salama K 2007 *Supercond. Sci. Technol.* **20** S147

[10] Haugan T, Barnes P N, Wheeler R, Meisenkothen F and Sumption M 2004 *Nature* **430** 867

[11] MacManus-Driscoll J L, Foltyn S R, Jia Q X, Wang H, Serquis A, Maiorov B, Civale L, Lin Y, Hawley M E, Maley M P and Peterson D E 2004 *Appl. Phys. Lett.* **84** 5329

[12] Barnes P N, Kell J W, Harrison B C, Haugan T J, Varanasi C V, Rane M and Ramos F 2006 *Appl. Phys. Lett.* **89** 012503

[13] Pradhan A K, Muralidhar M, Feng Y, Murakami M, Nakao K and Koshizuka N 2000 *Appl. Phys. Lett.* **77** 2003

[14] Li L W, Cao S X, Li W F, Liu F, Chi C Y, Jing C and Zhang J C 2005 *Acta Phys. Sin.* **54** 3839 (in Chinese)

[15] Li P L, Wang Y Y, Tian Y T, Wang J, Niu X L, Wang J X, Wang D D and Wang X X 2008 *Chin. Phys.* B **17** 3484

[16] Lee S Y, Song S and Kim B J 2006 *Physica* C **445–448** 578

[17] Nakaoka K, Matsuda J, Kitoh Y, Goto T, Yamada Y, Izumi T and Shiohara Y 2007 *Physica* C **463–465** 519

[18] Feldmann D M, Ugurlu O, Maiorov B, Stan L, Holesinger T G, Civale L, Foltyn S R and Jia Q X 2007 *Appl. Phys. Lett.* **91** 162501

[19] Chen Z, Kametani F, Kim S I, Larbalestier D C, Jang H W, Choi K J and Eom C B 2008 *J. Appl. Phys.* **103** 043913

[20] Kim H S, Song B, Kwon N Y, Kim K L and Lee H G 2009 *Supercond. Sci. Technol.* **22** 125016

[21] Dam B, Huijbregtse J M, Klaassen F C, Geest R F, Doornbos G, Rector J H, Testa A M, Freisem S, Martinezk J C, Stäuble-Pümpin B and Griessen R 1999 *Nature* **399** 439